

Article

# Backstepping Sliding Mode Control of a Permanent Magnet Synchronous Motor Based on a Nonlinear Disturbance Observer

Jiandong Duan , Shuai Wang and Li Sun

School of Electrical Engineering and Automation, Harbin Institute of Technology, Harbin 150001, China

\* Correspondence: duanjiandong1985@126.com

**Abstract:** In this paper, a backstepping sliding mode controller based on a nonlinear disturbance observer (NDO-SMC) is proposed to realize the high-performance speed control of a permanent magnet synchronous motor (PMSM). This paper compares the advantages and disadvantages of the traditional backstepping sliding mode control algorithm (SMC) and integral backstepping sliding mode control algorithm (I-SMC) in the face of mismatched disturbances. In view of the shortcomings of these two algorithms, the idea of using a disturbance observer to observe disturbance and carry out dynamic compensation is proposed, and the composite controller is designed. The overshoot and settling time is improved by 30% and 8 s, respectively, for the proposed NDO-SMC controller compared with the SMC controller. The simulation and experimental results illustrate that the designed controller not only effectively solves the torque jitter problem of SMC, but also improves the overshoot problem caused by the integral module of I-SMC. There is also a better matching degree between the theoretical derivation, the simulation results, and experimental data. It also proves that the composite control algorithm proposed in this paper provides a meaningful solution to the operation disturbance suppression problem of the permanent magnet synchronous motor.

**Keywords:** PMSM control; backstepping sliding mode controller; nonlinear disturbance observer



**Citation:** Duan, J.; Wang, S.; Sun, L. Backstepping Sliding Mode Control of a Permanent Magnet Synchronous Motor Based on a Nonlinear Disturbance Observer. *Appl. Sci.* **2022**, *12*, 11225. <https://doi.org/10.3390/app122111225>

Academic Editor:  
Georgios Papadakis

Received: 7 October 2022  
Accepted: 4 November 2022  
Published: 5 November 2022

**Publisher's Note:** MDPI stays neutral with regard to jurisdictional claims in published maps and institutional affiliations.



**Copyright:** © 2022 by the authors. Licensee MDPI, Basel, Switzerland. This article is an open access article distributed under the terms and conditions of the Creative Commons Attribution (CC BY) license (<https://creativecommons.org/licenses/by/4.0/>).

## 1. Introduction

The permanent magnet synchronous motor (PMSM) has been widely used in modern industrial fields because of its advantages of having a small size, simple design, high efficiency, and high power density, and it is used in many applications such as numerically controlled machine tools, robots, new energy vehicles, and other fields [1]. In the operation process of PMSM, there are factors such as current coupling, magnetic field saturation, and external or internal unknown interference, which make the motor to become a highly nonlinear system [2]. Therefore, obtaining high-performance control algorithms has become the key to PMSM applications. In recent years, with the development of modern control theory and power electronics technology, many researchers have developed a large number of PMSM control strategies and control algorithms. The main control strategies are magnetic field directional control (FOC), direct torque control (DTC), maximum torque per ampere (MTPA), etc. The control algorithms are used for the specific implementation to design the controllers in each control strategy. At present, the most widely used control strategy is the FOC, because it can effectively realize the decoupling of the stator current [3]. After the development and application of the FOC strategy, the main problem that restricts the control performance of PMSM becomes how to solve the impact of the external or internal unknown disturbances. The internal disturbance of PMSM mainly includes motor parameter variation [4], back electromotive force, and torque ripple [5], and the external disturbance mainly refers to load torque disturbance [6].

In order to solve the disturbance problem, researchers have proposed different control algorithms, such as the PID control algorithm, sliding mode control algorithm, backstepping

control algorithm, adaptive control algorithm, robust control algorithm, neural network control algorithm, and fuzzy control algorithm [7–12]. Among them, the PID control algorithm is the longest and most widely used control algorithm. The control structure of the PID control algorithm is simple and easy to use, and the integral loop itself can suppress special types of disturbances. However, the PID control algorithm is a linear algorithm, and it also has the shortcomings of a linear algorithm, that is, there is a contradiction between the overshoot of the system dynamic response and the settling time [13]. In addition, the response speed of the traditional PID controller to suppress disturbances is dependent on its parameters, and although there are many tuning algorithms that have improved the performance of traditional PID controllers, it is difficult for traditional PID controllers to ensure zero steady-state error control under time-varying parameter disturbance [14].

Among the remaining control algorithms listed above, backstepping algorithm and sliding mode algorithm are the control algorithms that researchers pay most attention to [15]. The backstepping algorithm is widely recognized because it is a control algorithm with self-stabilization and wide relaxation matching conditions. Under the semi-accurate conditions of the PMSM model, the backstepping algorithm is a control algorithm that is closest to the essence of the PMSM motor model. In addition, the q-axis model of the PMSM is a second-order model, and the backstepping method can connect the second-order models like a bridge and ensure that each order state is asymptotically stable in the global scope [16,17]. The sliding mode control algorithm has a simple structure, and more importantly, it has a strong disturbance rejection capability [18]. However, the sliding mode surface of the traditional sliding mode control algorithm is mostly designed as a linear sliding mode surface, which makes the sliding mode control algorithm more sensitive to model mismatch and unknown disturbances [19]. For the problems of sliding mode control, the current research is generally divided into two categories: The first category mainly uses some classic control design tools, such as using the Riccati inequation method to design a new type of sliding surface [20], to study the robust stability of various systems under mismatched uncertainties. The sliding mode controller designed based on the above method must require that these model mismatch and unknown disturbances must be bounded by the  $H_2$  norm, that is to say, these unmatched disturbances must belong to the self-decaying disappearance type. Taking PMSM as an example, the load torque and the mismatched parameters disturbance therein may have nonzero steady-state values and thus do not have bounded  $H_2$  norms [21]. The second method is to add an integral module to the traditional sliding mode controller to construct an integral sliding mode controller [22]. The design idea of the integral sliding mode control algorithm is to design a high-frequency switching gain to force the state to achieve an integral sliding surface. When matching the unknown disturbance action, the integral action of the sliding surface drives the state to the desired equilibrium state. Compared with the first type of mismatch uncertainty, the integral sliding mode control algorithm has received more attention from researchers because of its simplicity and robustness. Of course, the integral action will often bring some adverse effects to the control system, such as a large overshoot and long transition time [23]. In [24,25], the authors proposed nonsingular integral terminal sliding mode control, which guarantees fast transient convergence both at a distance from and at a close range to the equilibrium point. The above two types of SMC methods use a robust way to suppress the influence of the model mismatch and unknown disturbances, which means that the attenuation of the model mismatch and unknown disturbances is at the expense of the performance of the PMSM servo control system. In addition, the torque jitter of the sliding mode control algorithm itself is still an urgent problem to be solved [26].

The main research contents of this paper are as follows: Based on *Lyapunov's* second stability theory, a backstepping sliding mode controller and a backstepping integral sliding mode controller are designed, and the control performance of the two control algorithms in the face of model mismatch and unknown disturbances is compared. Aiming at the deficiencies of the two types of sliding mode control algorithms, a nonlinear disturbance observer is designed and a backstepping sliding mode composite controller based on the

nonlinear disturbance observer is constructed. The design idea is to offset or weaken the negative influence of the model mismatch and unknown disturbances in the PMSM servo system on the dynamic response of the system through the nonlinear disturbance observer.

The second chapter of this paper establishes the basic mathematical model of PMSM and describes the feedback system. Section 3 designs two types of sliding mode controllers and nonlinear disturbance observers, and proves the stability of the back-step sliding mode composite control system based on nonlinear disturbance observers. Section 4 gives the simulation experiments. Section 5 is the conclusion of this article.

### 2. Mathematical Model of PMSM

It is assumed that the magnetic circuit of the permanent magnet synchronous motor is not saturated, the hysteresis and eddy current loss are ignored, and the distribution of the magnetic field is assumed to be a sinusoidal space. In this case, the ideal mathematical model of the surface mount permanent magnet synchronous motor is expressed in the  $d$ - $q$  coordinates, as follows [27]:

$$p \begin{bmatrix} i_d \\ i_q \\ \omega \end{bmatrix} = \begin{bmatrix} -\frac{R_s}{L_d} & n_p\omega & 0 \\ -n_p\omega & -\frac{R_s}{L_q} & -\frac{n_p\psi_f}{L_q} \\ 0 & \frac{3n_p\psi_f}{2J} & -\frac{B}{J} \end{bmatrix} \begin{bmatrix} i_d \\ i_q \\ \omega \end{bmatrix} + \begin{bmatrix} \frac{u_d}{L_d} \\ \frac{u_q}{L_q} \\ -\frac{T_L}{J} \end{bmatrix} \tag{1}$$

where  $R_s$  represents the stator resistance,  $u_d$  and  $u_q$  presents the stator voltage of the  $d$ - $q$  axis,  $i_d$  and  $i_q$  represents the stator current of the  $d$ - $q$  axis, and  $L_d$  and  $L_q$  represents the synchronous inductance of the  $d$ - $q$  axis. The research object of this article is a surface mount permanent magnet synchronous motor, so  $L_d = L_q = L$ .  $n_p$  represents the number of pole pairs of the permanent magnet synchronous motor,  $\omega$  represents the rotor angular velocity of the motor,  $\psi_f$  represents the permanent magnet flux linkage,  $T_L$  represents the load torque,  $B$  represents the viscous friction coefficient, and  $J$  represents the rotor inertia.

The block diagram of the permanent magnet synchronous motor servo speed control system is shown in Figure 1. The entire servo speed control system consists of a permanent magnet synchronous motor with load, a space vector pulse width modulation module (SVPWM), a voltage source inverter, and two controllers based on a field-oriented strategy. Among them, the  $d$ -axis controller adopts the  $i_d = 0$  control strategy. As this article mainly studies the speed control of permanent magnet synchronous motors, the  $d$ -axis controller is designed as a PI controller, and the PI controller is used to stabilize the  $d$ -axis current. The  $q$ -axis controller is a back-step sliding mode controller. The disturbance observer is used to feed the observed mismatch disturbance to the controller.

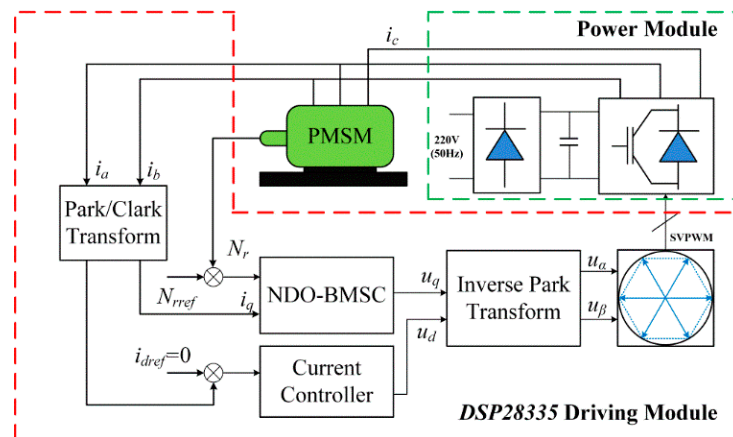


Figure 1. PMSM servo speed control system.

### 3. Control Strategy Description

#### 3.1. Description of the Feedback System

In order to make the mathematical derivation process of the whole article clearer and clearer, rewrite the q-axis state equation in Equation (1) into the following form:

$$\begin{aligned} \dot{x}_1 &= ax_1 + bx_2 + d(t) \\ \dot{x}_2 &= cx_1 + dx_2 + gu \\ y &= x_1 \end{aligned} \tag{2}$$

Among them,

$$a = -\frac{B}{J}; b = \frac{3P\psi}{2J}; c = -\frac{P\psi}{L}; d = -\frac{R}{L}; g = \frac{1}{L}; x_1 = \omega; x_2 = i_q$$

and  $d(t)$  is the aggregate disturbances of the mismatched channels of the PMSM system.

The research goal of this paper is to realize the speed tracking control of PMSM. Therefore, an error tracking control signal ( $e$ ) and an error control signal of disturbance ( $e_{d(t)}$ ) are defined in this section. The specific forms are as follows:

$$e = x_1 - x_{1d} \tag{3}$$

$$e_{d(t)} = d(t) - \hat{d}(t) \tag{4}$$

where  $\hat{d}(t)$  is the observer estimate value of  $d(t)$  and  $x_{1d}$  represents the desired value of  $x$ . The significance of defining Equations (3) and (4) is that it can ensure that the speed of the PMSM servo control system converges to the desired value in a finite time, and the error estimate converges to the true value. Equation (5) is the state equation of the speed tracking control signal.

$$\begin{aligned} \dot{e} &= \dot{x}_1 - \dot{x}_{1d} = ax_1 + bx_2 + d(t) \\ &= a(e + x_{1d}) + bx_2 + d(t) \\ &= ae + ax_{1d} + bx_2 + d(t) \end{aligned} \tag{5}$$

Equations (3) and (5) can be solved simultaneously to obtain the  $q$ -axis state equation of the PMSM servo speed control system, as shown in Equation (6).

$$\begin{bmatrix} \dot{e} \\ \dot{x}_2 \end{bmatrix} = \begin{bmatrix} a & b \\ c & d \end{bmatrix} \begin{bmatrix} e \\ x_2 \end{bmatrix} + \begin{bmatrix} 0 \\ g \end{bmatrix} u + \begin{bmatrix} 1 \\ 0 \end{bmatrix} d(t) + \begin{bmatrix} a \\ c \end{bmatrix} x_{1d} \tag{6}$$

#### 3.2. Basic Theory of Sliding Mode Controller

In this paper, different sliding mode controllers are designed to realize the speed tracking control of PMSM. In the design process of the controller, the most traditional sliding mode surface is generally designed as a linear sliding mode surface, and its expression is as follows:

$$s = c_1 e + x_2 \tag{7}$$

where  $s$  represents the sliding mode surface function and  $c_1$  is the parameter of the sliding mode surface, and its value cannot be zero. In order to achieve the strong robustness of the PMSM servo system, and to ensure the study of this paper does not lose generality, this paper selects the constant approximation law, and obtains the state equation of sliding surface as shown in Equation (8):

$$\dot{s} = c_1 \dot{e} + \dot{x}_2 \tag{8}$$

The control output signal of the design backstepping sliding mode controller is as follows:

$$u = -g^{-1}[(ac_1 + c)e + (bc_1 + d)x_2 + (ac_1 + c)x_{1d} + K\text{sgn}(s)] \tag{9}$$

where  $K$  is the constant velocity approach rate switching gain parameter.

Combining Equations (6)–(9), the sliding mode surface function is derived as follows:

$$\dot{s} = -K\text{sgn}(s) + c_1\dot{d}(t) \tag{10}$$

Equation (10) can be analyzed, if the value of the switching gain parameter of the constant velocity approach rate is greater than  $\|c_1\dot{d}(t)\|$ , the q-axis sliding mode surface equation of the PMSM can converge to zero in a finite time. However, the prerequisite for this inference is to ensure that the disturbance of the system mismatched channel is bounded. Although this condition makes the sliding mode control algorithm have some limitations, compared with the rest of the nonlinear algorithm, the condition of the bounded disturbance is more in line with the actual operating conditions of the PMSM constraints, which is one of the reasons the sliding mode control is widely used.

The steady-state equation of the speed tracking control signal can be obtained by introducing  $s = 0$  into Equation (6) as follows:

$$\dot{e} = (a - bc_1)e + ax_{1d} + \dot{d}(t) \tag{11}$$

The analysis of Equation (11) shows that the designed backstepping sliding mode controller can make the speed reach the sliding surface in a limited time, but the equilibrium point calculated by the equation is not the origin, which indicates that the system cannot reach the desired sliding surface. The system will only vibrate near the sliding surface. This inference also proves that the sliding mode control algorithm has a good suppression effect on the disturbance of the matched channel, but is more sensitive to the influence of the disturbance of the unmatched channel.

### 3.3. Design of Backstepping Integral Sliding Mode Controller

In order to solve the problem that the traditional backstepping sliding mode control algorithm is more sensitive to the disturbance of the unmatched channel, this chapter designs a backstepping integral sliding mode controller. The sliding mode surface is designed as follows:

$$s = c_1e + x_2 + c_2 \int e dt \tag{12}$$

where  $c_2$  is the parameter of the sliding mode surface, and its value cannot be zero. The state equation of the sliding surface is shown in Equation (13).

$$\dot{s} = c_1\dot{e} + \dot{x}_2 + c_2e \tag{13}$$

Choose the constant approximation law to design the controller, and the control output signal is shown in Equation (14).

$$u = -g^{-1}[(ac_1 + c + c_2)e + (bc_1 + d)x_2 + (ac_1 + c)x_1\dot{d} + K\text{sgn}(s)] \tag{14}$$

Substituting the designed control output signal expression (14) into Equation (6), and at the same time, we can obtain the following Equation:

$$\ddot{e} + (bc_1 - a)\dot{e} + bc_2e = a\dot{x}_{1d} + \ddot{d}(t) \tag{15}$$

In the PMSM speed control system, the desired value of the speed is set as a constant, so that Equation (15) can be simplified into Equation (16).

$$\ddot{e} + (bc_1 - a)\dot{e} + bc_2e = \dot{d}(t) \tag{16}$$

Analyzing Equation (16) can prove that if the disturbance is a parameter that changes very slowly with time, then the equilibrium point of the system will converge to the origin. In other words, the speed of the PMSM will also converge to the sliding surface in a limited time, thereby realizing the tracking control of the speed. The backstepping

integral sliding mode controller can effectively eliminate the steady-state bias caused by the system mismatched channel disturbance, and the entire PMSM speed control system has better robustness. However, in addition to the above-mentioned advantageous factors, the addition of the integral mode will greatly increase the adjustment time of the system and bring about a larger overshoot.

### 3.4. Design of the Disturbance Observer and Compound Controller

In the analysis of the previous section, although the introduction of the integration module in the design of the sliding mode control system can reduce the sensitivity of the system to mismatched channel disturbances, the prerequisite for this control performance is that the disturbance is a slowly varying variable. Therefore, it is difficult to achieve high-performance speed tracking control by relying only on the I-SMC when the system is subject to continuous abrupt disturbances. In this section, a nonlinear disturbance observer is designed to compensate the disturbance, and the specific design process is as follows:

Rewriting Equation (6) as an observation Equation, as shown in Equation (17):

$$\begin{aligned} \dot{z} &= f(z) + \lambda_1 u + \lambda_2 d(t) + \omega, \\ \lambda_1 &= [0 \quad g]^T, \lambda_2 = [1 \quad 0]^T. \end{aligned} \tag{17}$$

where  $z$  is the observed state quantity. When the system is in a steady state, there is  $\dot{z} = 0$ , and then Equation (17) can be simplified to Equation (18).

$$-\lambda_2 d(t) = f(z) + \lambda_1 u + \omega \tag{18}$$

$$\text{Let } \hat{d}(t) = p + lz$$

The nonlinear disturbance observer is designed as follows:

$$\begin{cases} \dot{p} = -lp - l[\lambda_2 lz + f(z) + \lambda_1 u + \omega] \\ \hat{d}(t) = p + lz \end{cases} \tag{19}$$

where  $p$  is the observer state parameter, and  $l$  is the observer gain parameter, whose value is a constant greater than zero. The matrix form of the observer is shown in Equation (20).

$$\begin{bmatrix} \dot{p}_1 \\ \dot{p}_2 \end{bmatrix} = \begin{bmatrix} -l_1 p_1 \\ 0 \end{bmatrix} - \begin{bmatrix} l_1^2 e \\ 0 \end{bmatrix} - \begin{bmatrix} l_1 & 0 \\ 0 & l_2 \end{bmatrix} \left\{ \begin{bmatrix} a & b \\ c & d \end{bmatrix} \begin{bmatrix} e \\ x_2 \end{bmatrix} + \begin{bmatrix} 0 \\ g \end{bmatrix} u + \begin{bmatrix} a \\ c \end{bmatrix} x_1 d \right\} \tag{20}$$

The disturbance of the mismatched channel is input into the controller in the form of feedback, and then the NOD-SMC controller is constructed. The control output signal is shown in Equation (21):

$$u = -g^{-1} \left[ (ac_1 + c)e + (bc_1 + d)x_2 + (ac_1 + c)x_{1d} + \hat{d}(t) + K \text{sgn}(s) \right] \tag{21}$$

### 3.5. Stability Analysis

The minimum control requirement is to ensure that the system is globally stable for dynamic systems. In this paper, the traditional SMC uses a constant approximation law, which is equivalent to linearizing the system in a local range and achieving global uniformity and bounded stability. This section mainly analyzes the stability of the PMSM control system under the action of the backstepping sliding mode controller based on the nonlinear disturbance observer. The specific analysis process is as follows:

First, explain the state parameters and variables to be used. The new sliding mode face equation of state is shown in Equation (22):

$$\begin{aligned} \dot{s} &= c_1 \dot{e} + \dot{x}_2 + \hat{d}(t) \\ &= c_1 [ax_1 + bx_2 + d(t)] + cx_1 + dx_2 + gu + \hat{d}(t) \end{aligned} \tag{22}$$

Substituting Equation (21) into Equation (22):

$$\dot{s} = -K\text{sgn}(s) + c [d(t) - \hat{d}(t)] + \hat{d}(t) \tag{23}$$

where

$$\dot{\hat{d}}(t) = -l\lambda_2 [\hat{d}(t) - d(t)]$$

Equation (23) can be further simplified to Equation (24).

$$\dot{s} = -K\text{sgn}(s) + (c + l\lambda_2)ed(t) \tag{24}$$

Then, construct the Lyapunov function of the system as Equation (25) and the derivative function of the *Lyapunov* function as Equation (26).

$$v = \frac{1}{2}s^2 \rightarrow PD \tag{25}$$

$$\dot{v} = s\dot{s} = [-K\text{sgn}(s) + (c + l\lambda_2)e_{d(t)}] \cdot s \tag{26}$$

According to *Lyapunov's* second stability theory, if we want to ensure that the PMSM system is globally asymptotically stable, and we must make Equation (25) a positive definite function and Equation (26) is a negative definite function. Solving Equation (26) gives the following:

$$\begin{aligned} \dot{v} &= s\dot{s} = [-K\text{sgn}(s) + (c + l\lambda_2)e_{d(t)}] \cdot s \\ &= -K|s| + (c + l\lambda_2)e_{d(t)} \cdot s \end{aligned} \tag{27}$$

where  $\text{sgn}(s) = s/|s|, s \cdot \text{sgn}(s) = s/|s| = s^2/|s| = |s|$ .

$$\begin{aligned} \dot{v} &= s\dot{s} = -K|s| + (c + l\lambda_2)e_{d(t)} \cdot s \\ &\leq -K|s| + (c + l\lambda_2)|e_{d(t)}| \cdot |s| \\ &= -[K - (c + l\lambda_2)|e_{d(t)}|] \cdot |s| \end{aligned} \tag{28}$$

Equation (25) can be calculated, such that  $\frac{1}{2}s^2 = v \Rightarrow |s| = \sqrt{2}\sqrt{v}$ ,

$$\dot{v} = s\dot{s} \leq -\sqrt{2}[K - (c + l\lambda_2)|e_{d(t)}|] \cdot \sqrt{v} \tag{29}$$

If the value of  $K$  is greater than  $(c + l\lambda_2)|e_{d(t)}|$ , then Equation (27) can be simplified to the following Equation:

$$\dot{v} \leq -\eta\sqrt{v} \tag{30}$$

As Equation (25) proves  $v(t)$  to be a positive definite function,  $v(t)^{1/2}$  is still a positive definite function. If  $K$  takes the appropriate value, then  $\eta$  is a constant greater than zero, so Equation (30) shows that  $\dot{v}(t)$  is a negative definite function. In other words, the PMSM servo speed control system based on the nonlinear disturbance observer is globally asymptotically stable.

#### 4. Simulation and Experimental Results Analysis

This article carries on the simulation experiment under the PLECS environment. The parameters of the PMSM used in the simulation are shown in Table 1. This simulation experiment mainly verifies the control performance of the system under the action of the traditional sliding mode control algorithm, integral sliding mode control algorithm, and sliding mode control algorithm based on the disturbance observer. The experimental test platform is shown in Figure 2 and the experimental platform is described as follows: (i) A three-phase PMSM (MDMA302P1G) and its main parameters are presented in Table 1, (ii) a

high speed programmable dynamometer (Model DSP6001), (iii) a DC regulated power supply (IT6006C-800-25) is used as the DC power input of the system, and (iv) the switching frequency of the IGBT of the inverter is 10 KHz. Finally, the coordinate transformation as well as the proposed controller are implemented by means of a TMS320f28335 DSP control card.

**Table 1.** The main parameters of the PMSM.

Parameter	Symbol	Value	Unit
Rated voltage	$U$	200	V
Rated current	$I$	17.8	A
Rated speed	$\omega$	1000	r/min
Rated power	$P$	3	kW
Rated torque	$T_L$	14.3	Nm
Rotor inertia	$J$	0.003	kg·m <sup>2</sup>
Inductance	$L$	5.25	mH
Damping coefficient	$B$	0.008	Nms
Resistance	$R_s$	0.958	$\Omega$
No. of poles	$n_p$	4	

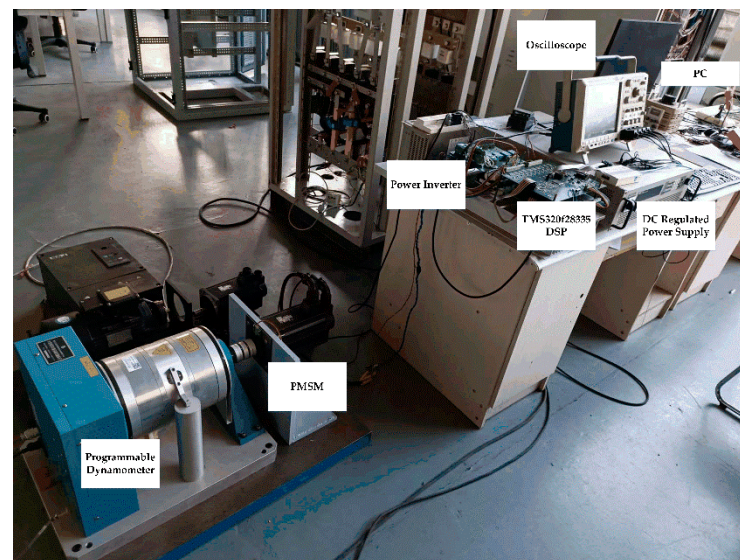


**Figure 2.** The experimental test platform.

#### 4.1. Simulation Analysis

Figure 3 shows the speed response waveform of PMSM. The simulation condition is that the 10 Nm load torque disturbance is added suddenly 0.5 s after a no-load start. From the figure, it can be seen that these three control algorithms perform very well in the PMSM speed tracking control. From the initial waveform within 0.2 s, it can be seen that although the integral sliding mode control algorithm has good steady-state characteristics, it brings a large overshoot to the system. This conclusion and the theoretical proof in Section 3 have a good match. In order to suppress this negative effect to the system due to insufficient control algorithms, this paper designs a sliding mode controller based on a nonlinear disturbance observer. It can be seen from the figure that the compound controller with a disturbance observer can compensate for the overshoot of the system to a certain extent. According to the detail drawings, it can be seen that when the system is disturbed by a sudden load, the traditional sliding mode algorithm has a constant steady-state bias. Although the integral sliding mode control brings a certain overshoot to the system, speed tracking control is the most basic requirement of the entire servo control system. In order to balance the dynamic performance of the system and the control target of the system at the same time, the sliding mode controller based on the nonlinear disturbance observer shows a more comprehensive and excellent performance.

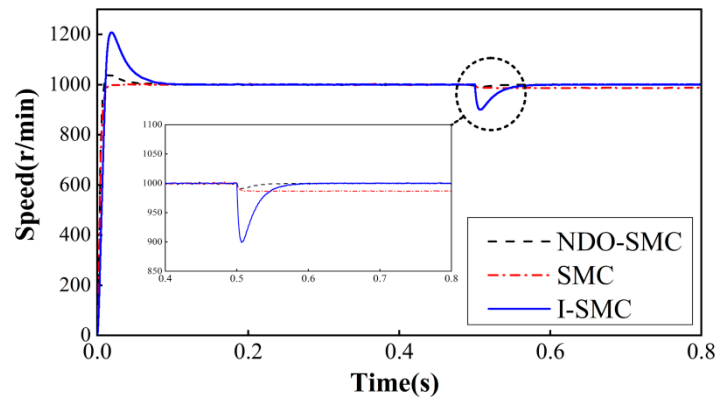


Figure 3. Speed response waveform of three controllers.

Figure 4 is the electromagnetic torque waveform of PMSM under the action of the NDO-SMC algorithm and I-SMC algorithm. It can be seen in Figure 4a that the electromagnetic torque waveform jitter of the sliding mode controller with disturbance observer compensation is small. Compared with Figure 4b, the electromagnetic torque jitter of the integral sliding mode controller without a disturbance observer is larger. In the occasions where a high performance is required, such a control performance is not allowed.

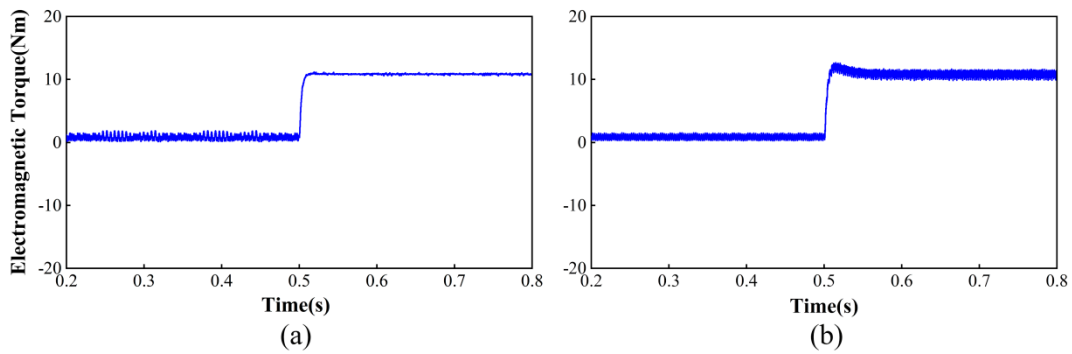


Figure 4. Electromagnetic torque of the (a) NOD-SMC controller and (b) I-SMC controller.

Figure 5 shows the PMSM stator three-phase current waveforms for both controllers. Comparing the current waveforms, it can be seen that the sliding mode controller based on the disturbance observer compensation has a higher sinusoidality for the three-phase currents and contains less harmonic currents, which in turn reduce the losses during PMSM operation [28].

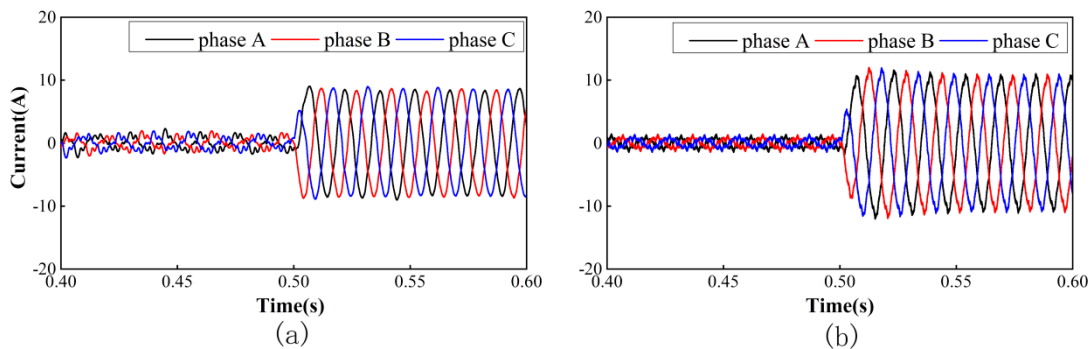


Figure 5. PMSM stator three-phase current waveforms of the (a) NOD-SMC controller and (b) I-SMC controller.

4.2. Experimental Analysis

Figure 6 shows the speed and current response waveforms of the three controllers. Figure 6a shows the no-load start waveform of the I-SMC. Figure 6b–d show the current and speed response for I-SMC, SMC, and NOD-SMC, respectively. From Figure 6, although the three controllers have different overshoots, it can be seen that all three controllers can achieve good speed tracking control under no-load conditions. However, after the motor is subjected to an impulse load torque of 10 Nm and an unknown disturbance in the mismatched channel, the three controllers show different responses. Although I-SMC still maintains speed tracking control for the motor, it produces almost the same amount of overshoot as at the no-load start up. In contrast, the dynamic characteristics of the latter two controllers are better. Figure 5 shows the response of the three controllers subjected to two disturbances. It can be seen from the figure species that the speed response of the SMC appears to have a constant static difference after being disturbed. The reason for this phenomenon is that the disturbance of the added mismatch channel is a constant. Therefore, although SMC has better dynamic performance than I-SMC, this steady-state static difference is fatal for high performance applications. In contrast, NOD-SMC combines the advantages of both controls, based on an observer, in order to identify unknown disturbances in the system, through the fast response time of a sliding mode controller. Ultimately, a PMSM high-performance speed control is achieved. This conclusion also matches well with the simulation in Figure 3. The transient response data for the three controllers are presented in Table 2.

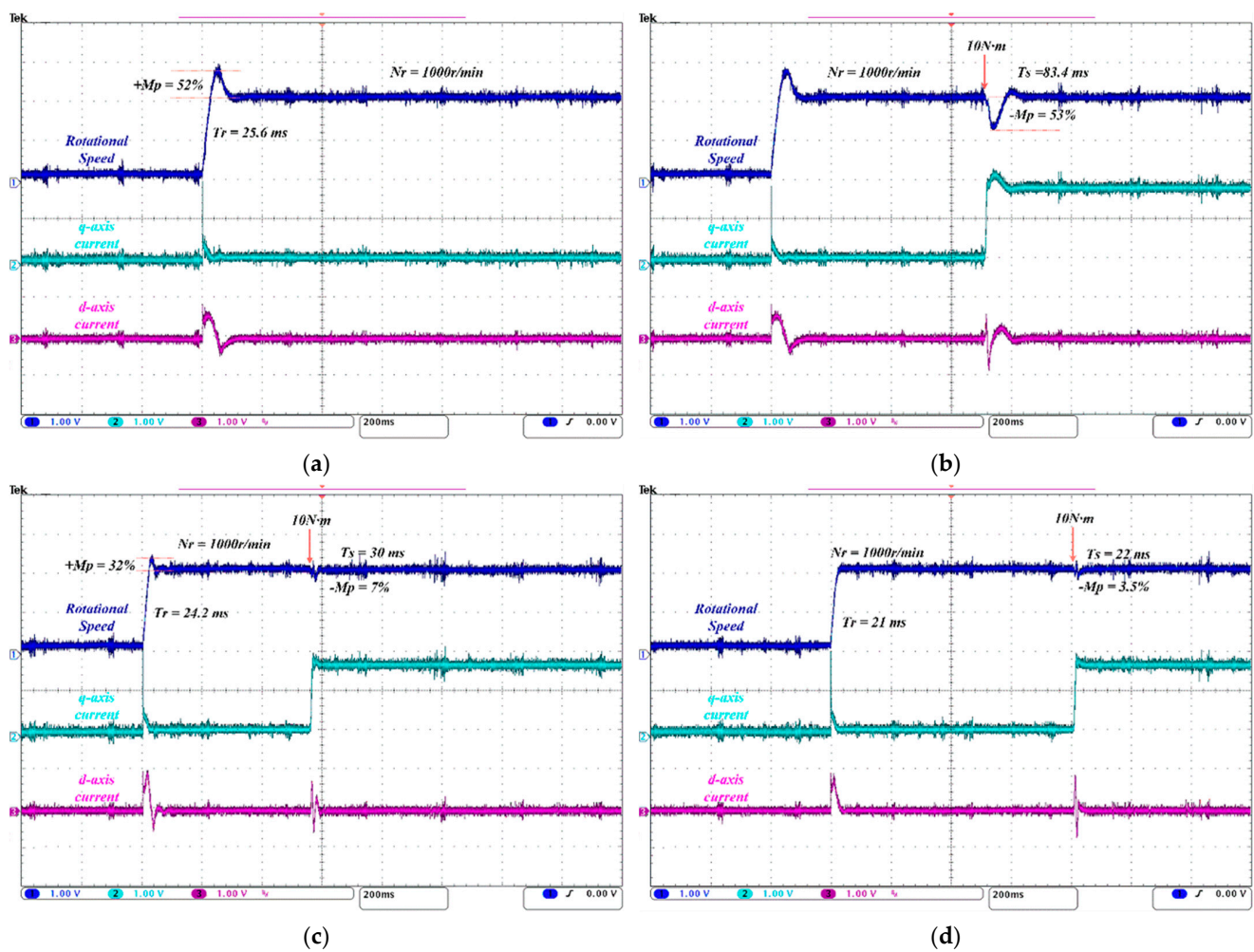
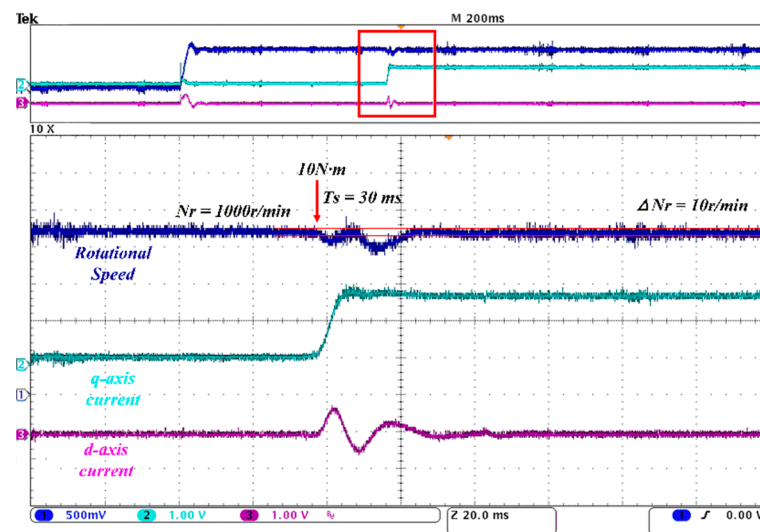


Figure 6. PMSM stator three phase current waveforms. (a,b) I-SMC, (c) SMC, and (d) NOD-SMC.

**Table 2.** The transient response data for the three controllers.

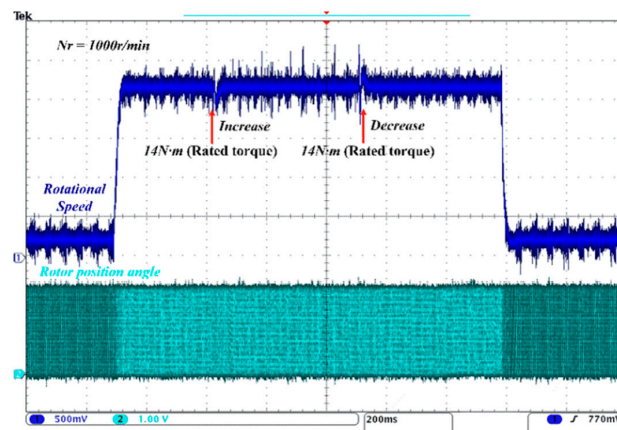
Controller	Mp (Start)	Mp (Load)	Rise Time (Tr/ms)	Settling Time (Ts/s)
I-SMC	+52%	−53.0%	25.6	83.4
SMC	+32%	−7.0%	24.2	30.0
NOD-SMC	+2%	−3.5%	21.0	22.0

Figure 7 shows the full operating response of the NOD-SMC. It consists of no-load starting of the motor to rated speed, followed by the sudden addition and reduction of the rated torque load, and no-load deceleration. Figure 7a,b shows that the rotor position angle does not fail or lose step even when the motor is disturbed by the rated torque, which also shows the robustness of the designed control system.



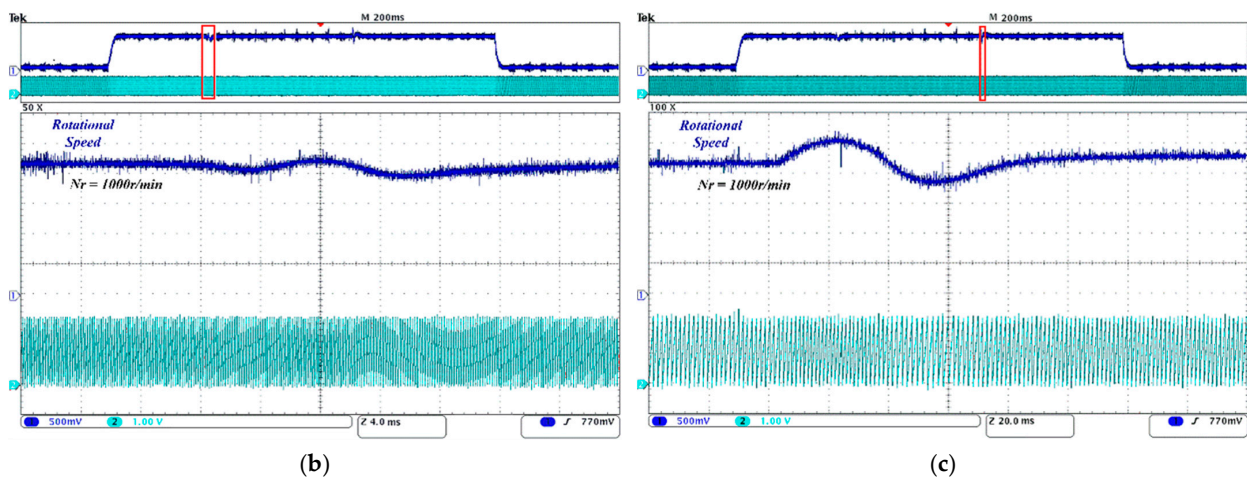
**Figure 7.** PMSM stator three phase current waveforms.

Figure 8 shows the complete speed waveform of the proposed controller, and it includes starting, increasing the rated load, reducing the load, and decelerating. Figure 8b,c shows the speed response for loading and decreasing the load, respectively. Although the speed fluctuates between two transient state processes with load changes, there is no missing or incorrect rotor position angle information. These waveforms not only prove the effectiveness of the proposed control algorithm, but also illustrate the correctness of the experiment platform.



(a)

**Figure 8.** Cont.



**Figure 8.** PMSM rotor position angle and speed waveforms. (a) Full working condition response waveform, (b) Speed response during loading, (c) Speed response at reduced load.

## 5. Conclusions

In this paper, a backstepping sliding mode composite controller based on a nonlinear disturbance observer is designed to realize the speed tracking control of the PMSM, and the advantages and disadvantages of the two kinds of sliding mode control algorithms in the face of sudden load disturbance are analyzed. Finally, it is proved that the composite controller designed in this paper can not only improve the disadvantages of the two controllers, but it also has a better dynamic performance.

The simulation and experimental test mainly verifies the speed response waveforms of the three controllers designed under the load torque sudden change, and proves that the sliding mode control is more sensitive to model mismatch and unknown disturbances, and at the same time causes the speed response to produce a steady-state bias. The second aspect proves that the integral module will also bring negative effects on the dynamic response of the system. Overall, the backstepping sliding mode composite controller based on a nonlinear disturbance observer has a smaller steady-state jitter and better dynamic response. The experimental results show that the control strategy is effective at suppressing the influence of model mismatch and unknown disturbances on the system during the operation of PMSM.

The proposed controller in this paper achieves a high performance speed tracking control of PMSM. The disturbance studied in this paper includes parameter perturbations and load torque. However, the effects caused by the parameter perturbations in the short-term experiments are not obvious during the experiments. In the future, further refinement of the disturbance types and more detailed disturbance models need to be established.

**Author Contributions:** J.D. proposed the idea and participated in the experiments and paper writing. S.W. completed the experimental work. L.S. and J.D. funded the experiment and revised the manuscript. J.D. and S.W. analyzed the results and wrote the paper. All authors have read and agreed to the published version of the manuscript.

**Funding:** This research was funded by the National Natural Science Foundation of China, grant number 52177211, and by the Heilongjiang postdoctoral research starting fund, grant number LBH-Q20020.

**Institutional Review Board Statement:** Not applicable.

**Informed Consent Statement:** Not applicable.

**Data Availability Statement:** Not applicable.

**Acknowledgments:** We thank Gao-Ru Chen for his suggestions regarding the experimental scheme of this paper.

**Conflicts of Interest:** The authors declare no conflict of interest.

## References

1. Tang, P.; Dai, Y.; Li, Z. Unified Predictive Current Control of PMSMs with Parameter Uncertainty. *Electronics* **2019**, *8*, 1534. [[CrossRef](#)]
2. Li, L.; Xiao, J.; Zhao, Y.; Liu, K.; Peng, X.; Luan, H.; Li, K. Robust position anti-interference control for PMSM servo system with uncertain disturbance. *China Electrotech. Soc. Trans. Electr. Mach. Syst.* **2020**, *4*, 151–160. [[CrossRef](#)]
3. Hoai, H.-K.; Chen, S.-C.; Than, H. Realization of the Sensorless Permanent Magnet Synchronous Motor Drive Control System with an Intelligent Controller. *Electronics* **2020**, *9*, 365. [[CrossRef](#)]
4. Lai, C.; Feng, G.; Mukherjee, K.; Kar, N.C. Investigations of the Influence of PMSM Parameter Variations in Optimal Stator Current Design for Torque Ripple Minimization. *IEEE Trans. Energy Convers.* **2017**, *32*, 1052–1062. [[CrossRef](#)]
5. Liu, Q.; Hameyer, K. Torque ripple minimization for direct torque control of PMSM with modified FCSMPC. *IEEE Trans. Ind. Appl.* **2016**, *52*, 4855–4864. [[CrossRef](#)]
6. Kuang, Z.; Du, B.; Cui, S.; Chan, C.C. Speed Control of Load Torque Feedforward Compensation Based on Linear Active Disturbance Rejection for Five-Phase PMSM. *IEEE Access* **2019**, *7*, 159787–159796. [[CrossRef](#)]
7. Hoai, H.-K.; Chen, S.-C.; Chang, C.-F. Realization of the Neural Fuzzy Controller for the Sensorless PMSM Drive Control System. *Electronics* **2020**, *9*, 1371. [[CrossRef](#)]
8. Wang, Y.; Feng, Y.; Zhang, X.; Liang, J. A New Reaching Law for Anti-disturbance Sliding-mode Control of PMSM Speed Regulation System. *IEEE Trans. Power Electron.* **2020**, *35*, 4117–4126. [[CrossRef](#)]
9. Sun, X.; Yu, H.; Yu, J.; Liu, X. Design and implementation of a novel adaptive backstepping control scheme for a PMSM with unknown load torque. *IET Electr. Power Appl.* **2019**, *13*, 445–455. [[CrossRef](#)]
10. Junejo, A.K.; Xu, W.; Mu, C.; Ismail, M.M.; Liu, Y. Adaptive Speed Control of PMSM Drive System Based A New Sliding-Mode Reaching Law. *IEEE Trans. Power Electron.* **2020**, *35*, 12110–12121. [[CrossRef](#)]
11. Cai, R.; Zheng, R.; Liu, M.; Li, M.L. Robust Control of PMSM Using Geometric Model Reduction and  $\mu$ -synthesis. *IEEE Trans. Ind. Electron.* **2018**, *65*, 498–509. [[CrossRef](#)]
12. Yu, J.; Shi, P.; Dong, W.; Chen, B.; Lin, C. Neural Network-Based Adaptive Dynamic Surface Control for Permanent Magnet Synchronous Motors. *IEEE Trans. Neural Netw. Learn. Syst.* **2015**, *26*, 640–645. [[CrossRef](#)]
13. Jung, J.-W.; Leu, V.Q.; Do, T.D.; Kim, E.-K.; Choi, H.H. Adaptive PID Speed Control Design for Permanent Magnet Synchronous Motor Drives. *IEEE Trans. Power Electron.* **2015**, *30*, 900–908. [[CrossRef](#)]
14. Ding, Y.; Kang, E.; Wang, S.; Chen, G.; Liu, F. Disturbance suppression for PMSM by a nonlinear composite controller based on two-channel. *IET Electr. Power Appl.* **2020**, *14*, 31–40. [[CrossRef](#)]
15. Wang, Y.; Yu, H.T.; Feng, N.J.; Wang, Y.C. Non-cascade backstepping sliding mode control with three-order extended state observer for PMSM drive. *IET Power Electron.* **2020**, *13*, 307–316. [[CrossRef](#)]
16. Linares-Flores, J.; Garcia-Rodriguez, C.; Sira-Ramirez, H.; Ramirez-Cardenas, O.D. Robust Backstepping Tracking Controller for Low-Speed PMSM Positioning System: Design, Analysis, and Implementation. *IEEE Trans. Ind. Inform.* **2015**, *11*, 1130–1141. [[CrossRef](#)]
17. Liu, S.; Guo, X.; Zhang, L. Robust Adaptive Backstepping Sliding Mode Control for Six-phase Permanent Magnet Synchronous Motor Using Recurrent Wavelet Fuzzy Neural Network. *IEEE Access* **2017**, *5*, 14502–14515.
18. Almeida, J.M.; Loukianov, A.G.; Castañeda, J.M.C.; Dominguez, J.R. Robust sensorless observer-based adaptive sliding modes control of synchronous motors. *J. Frankl. Inst. Eng. Appl. Math.* **2018**, *355*, 3221–3248. [[CrossRef](#)]
19. Luo, S.; Gao, R. Chaos control of the permanent magnet synchronous motor with time-varying delay by using adaptive sliding mode control based on DSC. *J. Frankl. Inst. Eng. Appl. Math.* **2018**, *355*, 4147–4163. [[CrossRef](#)]
20. Chang, J.-L. Dynamic Output Integral Sliding-Mode Control With Disturbance Attenuation. *IEEE Trans. Autom. Control* **2009**, *51*, 2653–2658. [[CrossRef](#)]
21. Li, S.; Yang, J.; Chen, W.-H.; Chen, X. *Disturbance Observer-Based Control Methods and Applications*; CRC Press: Boca Raton, FL, USA, 2014; Chapter 9; pp. 137–138.
22. Zhao, Y.; Liu, X.; Yu, H.; Yu, J. Model-free adaptive discrete-time integral terminal sliding mode control for PMSM drive system with disturbance observer. *IET Electr. Power Appl.* **2020**, *14*, 1756–1765. [[CrossRef](#)]
23. Zhang, X.; Sun, L.; Zhao, K.; Sun, L. Nonlinear Speed Control for PMSM System Using Sliding-Mode Control and Disturbance Compensation Techniques. *IEEE Trans. Power Electron.* **2013**, *28*, 1358–1365. [[CrossRef](#)]
24. Li, T.; Liu, X.; Yu, H. Backstepping Nonsingular Terminal Sliding Mode Control for PMSM With Finite-Time Disturbance Observer. *IEEE Access* **2021**, *9*, 135496–135507. [[CrossRef](#)]
25. Lei, Q.; Zhang, W.D. Tracking Control of AUVs via AdaptiveFast Nonsingular Integral Terminal Sliding Mode Control. *IEEE Trans. Ind. Inform.* **2020**, *16*, 1248–1258.
26. Liu, J.; Li, H.; Deng, Y. Torque Ripple Minimization of PMSM Based on Robust ILC Via Adaptive Sliding Mode Control. *IEEE Trans. Power Electron.* **2018**, *33*, 3655–3671. [[CrossRef](#)]
27. Xu, J.-X.; Panda, S.; Pan, Y.-J.; Lee, T.H.; Lam, B. A modular control scheme for PMSM speed control with pulsating torque minimization. *IEEE Trans. Ind. Electron.* **2004**, *51*, 526–536. [[CrossRef](#)]
28. Yi, P.; Sun, Z.; Wang, X. Research on PMSM harmonic coupling models based on magnetic co-energy. *IET Electr. Power Appl.* **2019**, *13*, 571–579. [[CrossRef](#)]